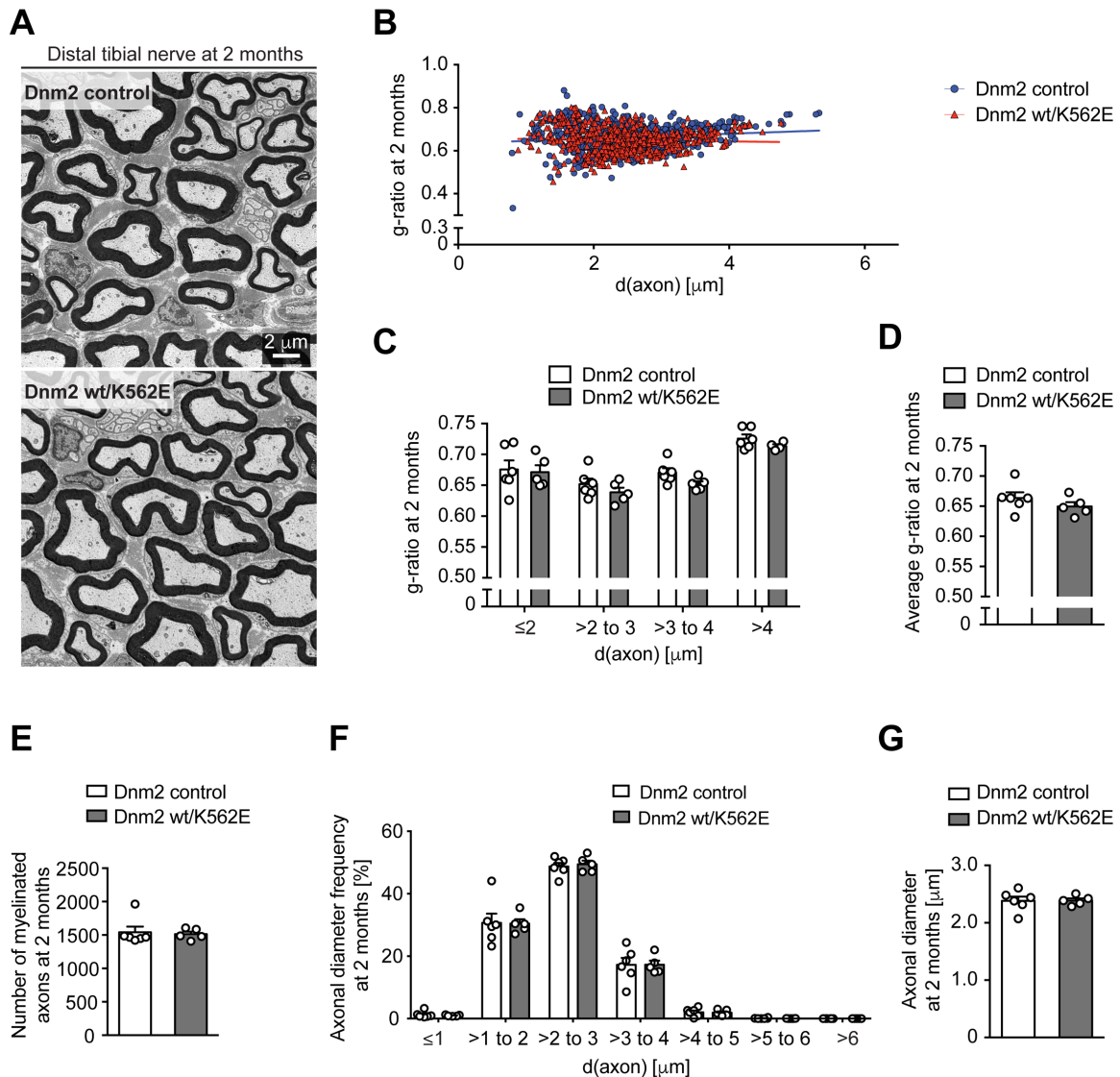


**Supplementary Material Figure S1: Normal myelin periodicity in Dnm2 wt/K562E mice.**

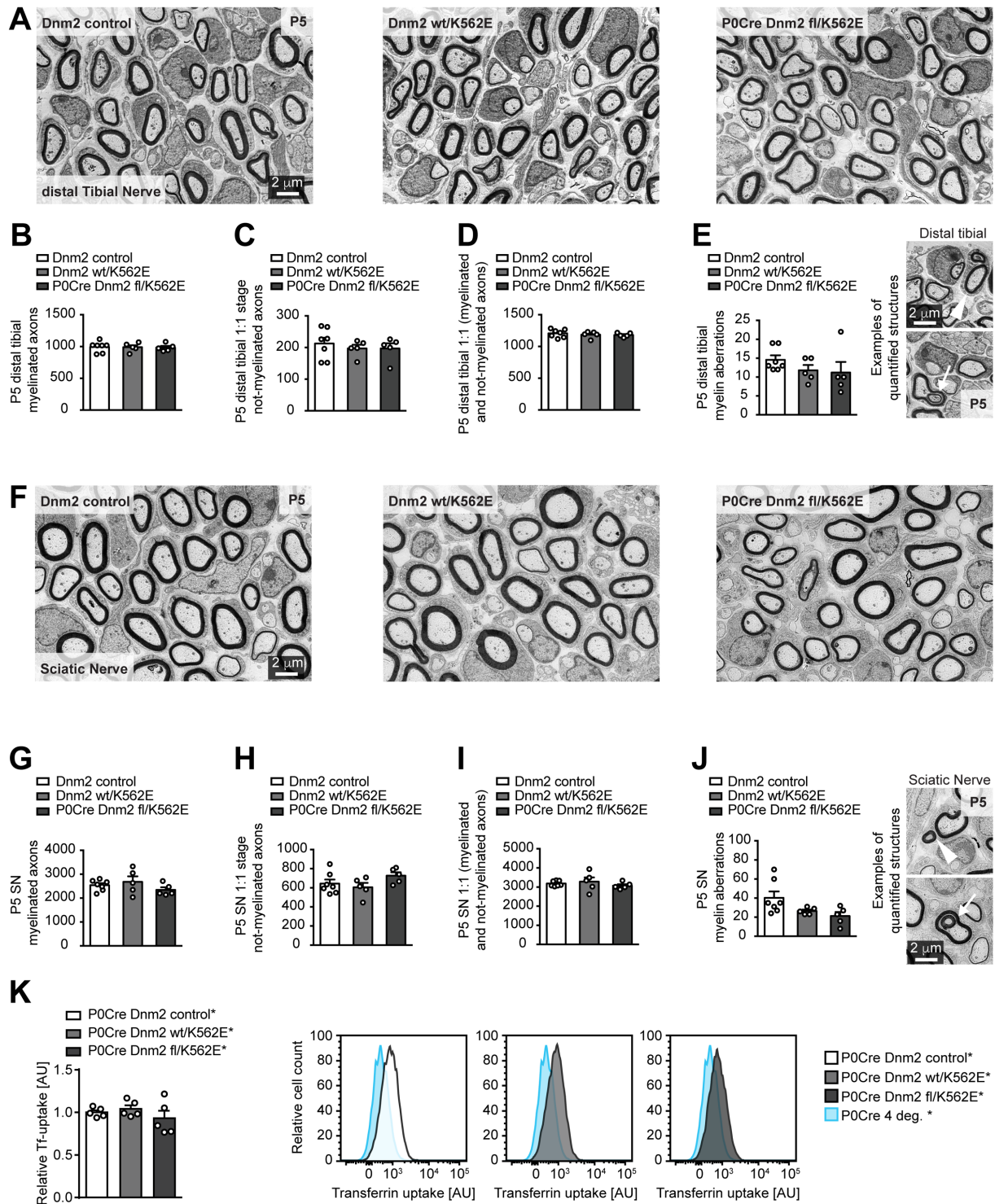
Exemplary EM pictures of myelin in distal tibial nerves from samples of 1 year-old control and Dnm2 wt/K562E mice were analysed for myelin periodicity, which is not significantly altered between both genotypes. Scale bar: 100nm, refers to whole panel. Bar heights: Mean; error bars: s.e.m. (n = 3 mice/genotype, 10 myelin sheaths per animal were analysed and averaged). Two-tailed unpaired Student's t-test.



**Supplementary Material Figure S2: No overt histological signs of a neuropathy on distal tibial nerves of Dnm2 wt/K562E mice at 2 months of age.**

(A) Exemplary EM pictures of distal tibial nerve cross sections of control and Dnm2 wt/K562E animals at 2 months. Scale bar: 2 $\mu\text{m}$ , refers to whole panel. (B) Scatter plot of g-ratio versus axonal diameter from measurements performed on distal tibial nerve EM micrographs derived from 2 months-old mice. Each datapoint represents one axon (n = 6 control and n = 5 Dnm2 wt/K562E mice, at least 97 axons were quantified per animal). (C, D) Binned g-ratio distribution per axonal diameter (C), and average g-ratio (D), of distal tibial nerves derived from 2 months-old mice (same nerves analysed as depicted in B). No significant differences were detected between g-ratios of both genotypes. Bar heights: Mean; error bars: s.e.m. (n = 6 control and n = 5 Dnm2 wt/K562E mice). (E to G) Number of myelinated axons (E), frequency distribution of axonal diameter bins (F), and average axonal diameter (G). All myelinated axons (E), and myelinated axons without myelin abnormalities (F, G), were measured in EM micrographs covering the entire cross-section of distal tibial nerves derived from 2 months-old mice. No

systematic changes in axonal diameters between Dnm2 wt/K562E and controls were detected. Bar heights: Mean; error bars: s.e.m. (n = 6 control and n = 5 Dnm2 wt/K562E mice). Two-Way ANOVA with Sidak's multiple comparisons test (**C**, **F**), two-tailed unpaired Student's t-test (**D**, **E**, **G**).

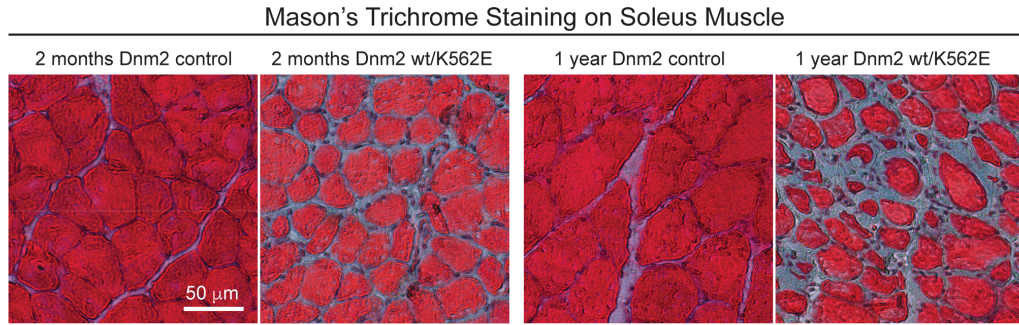
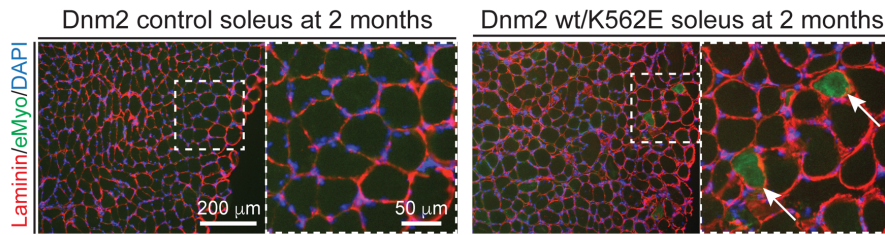
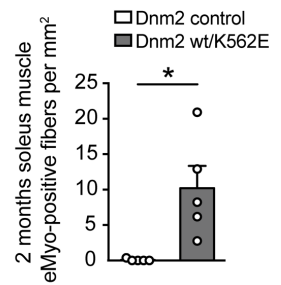
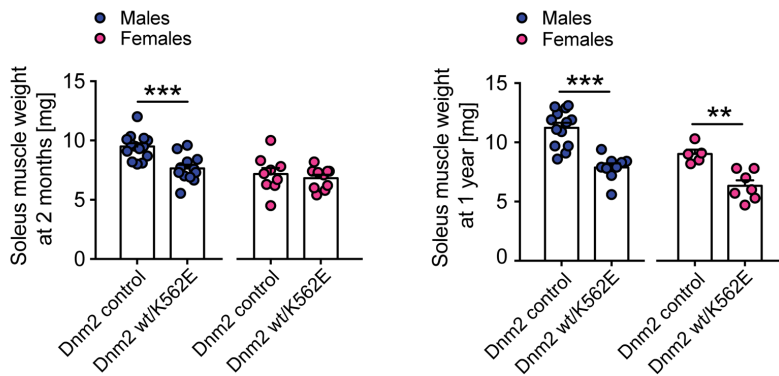
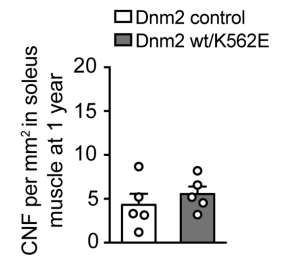


**Supplementary Material Figure S3: Excision of the wildtype allele from Schwann cells of DNM2 K562E-expressing mice does not significantly impair axon sorting and onset of myelination at P5.**

(A) Exemplary EM pictures of cross sections of distal tibial nerves of control, Dnm2 wt/K562E, and P0Cre Dnm2 fl/K562E at P5. Scale bar: 2 $\mu$ m, refers to whole panel. (B to D) Quantification of myelinated axons (B), and not-myelinated 1:1 SC-axon profiles (C) reveals no differences on the onset of myelination between control, Dnm2 wt/K562E and P0Cre Dnm2 fl/K562E distal



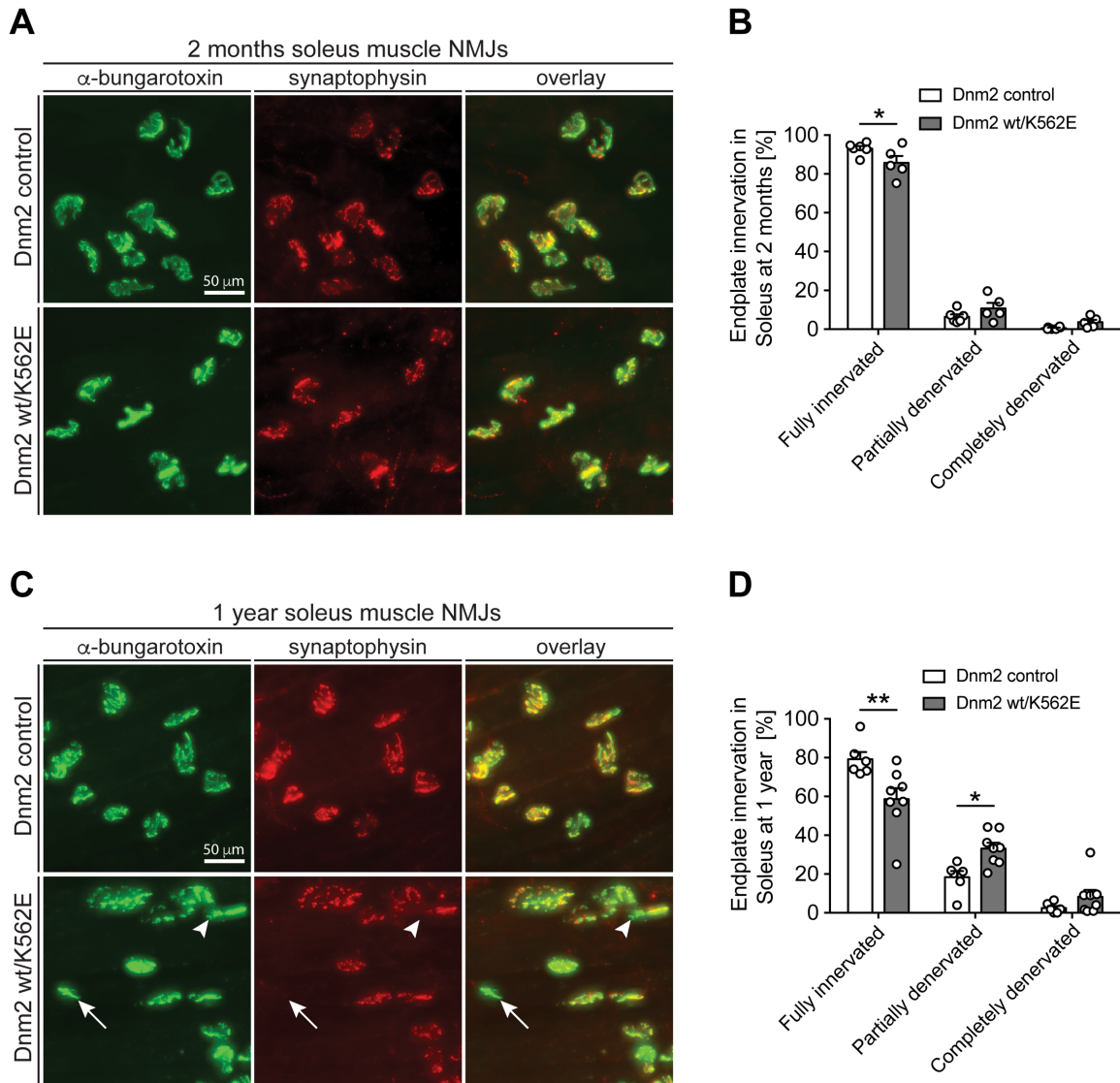
tibial nerves at P5. The total number of sorted axons (**D**, includes myelinated and not-myelinated 1:1 profiles) indicates no alterations on the outcome of radial sorting between control, Dnm2 wt/K562E and P0Cre Dnm2 fl/K562E distal tibial nerves. Whole cross-section EM panoramas were used for quantifications. Bar heights: Mean; error bars: s.e.m. (n = 7 control, n = 5 Dnm2 wt/K562E and P0Cre Dnm2 fl/K562E animals). (**E**) Evaluation of myelin abnormalities including outfoldings (white arrowhead) and infoldings (white arrow) throughout the entire cross-section of P5 distal tibial nerves in EM panoramas reveals no significant differences different between control, Dnm2 wt/K562E, and P0Cre Dnm2 fl/K562E mice. The images depicting examples of quantified structures derive from Dnm2 wt/K562E mice. Scale bar: 2 $\mu$ m, refers to whole panel. Bar heights: Mean; error bars: s.e.m. (n = 7 control, n = 5 Dnm2 wt/K562E and P0Cre Dnm2 fl/K562E animals). (**F**) EM micrographs of sciatic nerve cross sections of control, Dnm2 wt/K562E, and P0Cre Dnm2 fl/K562E at P5. Scale bar: 2 $\mu$ m, refers to whole panel. (**G to I**) Quantification of myelinated axons (**G**), and 1:1 not-myelinated SC-axon profiles (**H**) shows no differences in the onset of myelination between control, Dnm2 wt/K562E and P0Cre Dnm2 fl/K562E sciatic nerves at P5. The total number of sorted axons (**I**, includes myelinated and 1:1 not-myelinated) indicates no alterations on the outcome of radial sorting between control, Dnm2 wt/K562E and P0Cre Dnm2 fl/K562E sciatic nerves. Whole cross-section EM panoramas were used for quantifications. Bar heights: Mean; error bars: s.e.m. (n = 7 control, n = 5 Dnm2 wt/K562E and P0Cre Dnm2 fl/K562E animals). (**J**) Evaluation of myelin abnormalities including outfoldings (white arrowhead) and infoldings (white arrow) throughout the entire cross-section of P5 sciatic nerves in electron micrograph panoramas reveals no significant differences between control, Dnm2 wt/K562E and P0Cre Dnm2 fl/K562E mice. The images depicting examples of quantified structures derive from Dnm2 wt/K562E mice. Scale bar: 2 $\mu$ m, refers to whole panel. Bar heights: Mean; error bars: s.e.m. (n = 7 control, n = 5 Dnm2 wt/K562E and P0Cre Dnm2 fl/K562E animals). (**K**) FACS analyses of transferrin (Tf) uptake of YFP<sup>+</sup> primary mouse SCs derived from control\*, P0Cre Dnm2 wt/K562E\*, and P0Cre Dnm2 fl/K562E\*. Control SCs incubated at 4°C defines the baseline of the experiments. A profile of the 4°C condition is shown next to exemplary profiles derived from individual genotypes (right side). All genotypes contained P0Cre and the reporter ROSA eYFP (indicated by an \*) to ensure the FACS analysis was exclusive to SCs. (independent Schwann cell preparations were performed from every mouse, n = 5 mice/genotype). One-Way ANOVA with Tukey's multiple comparisons test.

**A****B****C****D****E**

### Supplementary Material Figure S4: Additional evidence for a myopathy in Dnm2 wt/K562E soleus muscles.

(A) Exemplary pictures of Mason's Trichrome-stained soleus muscle cryosections derived from control and Dnm2 wt/K562E mice at 2 months- and 1 year of age. Dnm2 wt/K562E soleus muscles display a wider extracellular-stained area in the mutant compared to control samples. (n = 5 mice per genotype, at least 3 pictures per mouse were acquired). Scale bar: 50μm, refers to whole panel. (B, C) Exemplary cryosections of soleus muscles from control and Dnm2 wt/K562E mice at 2 months of age probed with antibodies in (B) targeting laminin or embryonic myosin isoform (eMyo), and stained with DAPI. Exemplary eMyo-positive myofibers (white arrows) are highlighted. Scale bar: 200μm for the lower magnification images in the panel, and 50μm for the magnified images in the panel. Quantification of eMyo-positive myofibers (C) shows a significant increase in Dnm2 wt/K562E soleus muscles compared to controls. Bar

heights: Mean; error bars: s.e.m. (n = 5 mice/genotype, images from at least 3 sections quantified and averaged per mouse). **(D)** Analysis of soleus muscle weight (including the calcaneal tendon, used for handling the tissue) of control and Dnm2 wt/K562E sex-specific mice at 2 months- and 1 year of age. The muscles have a lower weight in Dnm2 wt/K562E males and females if compared to the respective controls at 1 year, a feature that is also significant in males at 2 months. Bar heights: Mean; error bars: s.e.m. (females at 2 months: n = 9 control and n = 10 Dnm2 wt/K562E; females at 1 year: n = 5 control and n = 7 Dnm2 wt/K562E; males at 2 months: n = 14 control and n = 12 Dnm2 wt/K562E; males at 1 year : n = 13 control and n = 9 Dnm2 wt/K562E). **(E)** Analysis of centronucleated fibers (CNF) in control and Dnm2 wt/K562E soleus muscle cryosections derived from 1 year-old mice reveals no significant changes between both genotypes. Bar heights: Mean; error bars: s.e.m. (n = 5 mice/genotype, images from 3 sections quantified and averaged per mouse). Two-tailed unpaired Student's t-test. Significance was set at \*p < 0.05, \*\*p < 0.01, \*\*\*p < 0.001.

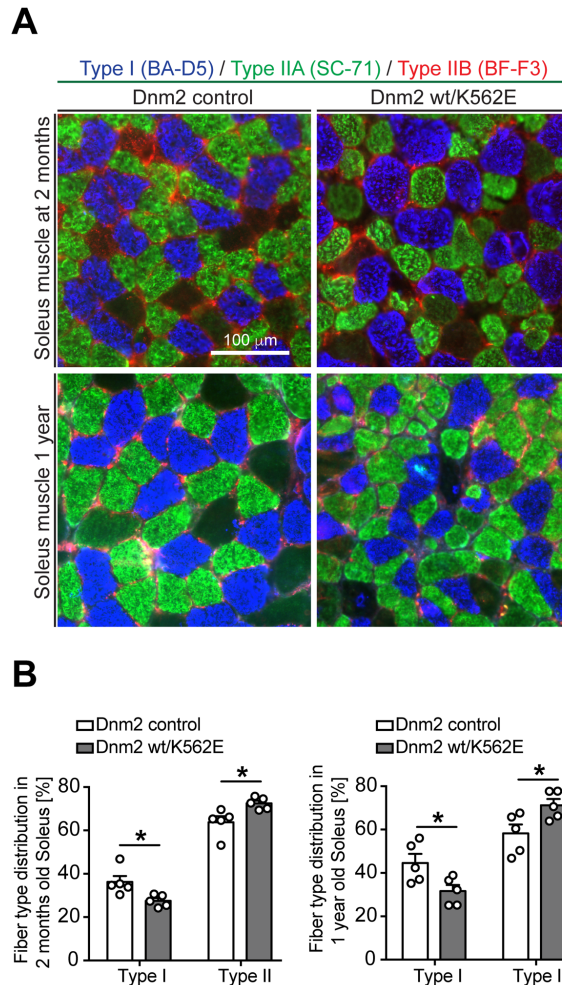


**Supplementary Material Figure S5: Neuromuscular junction analysis of Dnm2 wt/K562E soleus muscle does not show a significant increase in completely denervated endplates.**

(A, C) Exemplary images from whole-mount soleus muscle fibers with labelled neuromuscular junctions (NMJs) post-synaptic ( $\alpha$ -bungarotoxin) and pre-synaptic (synaptophysin) terminals derived from mice at 2 months (A) and 1 year of age (C). Examples of post-synaptic signals that are partially (white arrowhead) or completely (white arrow) not overlaid by the respective pre-synaptic signals are highlighted. Scale bar: 50 $\mu$ m, refers to whole panel. (B, D) Quantification of the NMJ endplates that are fully innervated, partially denervated or completely denervated at 2 months (B) and 1 year of age (D) shows no significant changes between control and Dnm2 wt/K562E mice in the number of fully denervated structures at both ages. The number of fully innervated NMJs are mildly reduced in mutants at both ages, and the partially denervated ones show a trend towards an increase in 2 months-old Dnm2 wt/K562E animals, which reaches statistical significance by 1 year of age. Bar heights: Mean; error bars:

s.e.m. (n = 6 control and n = 5 Dnm2 wt/K562E mice (2 months), n = 6 control and n = 8 Dnm2 wt/K562E mice (1 year), at least 100 neuromuscular junctions from each animal were quantified). Two-Way ANOVA with Sidak's multiple comparisons test. Significance was set at \*p < 0.05, \*\*p < 0.01.

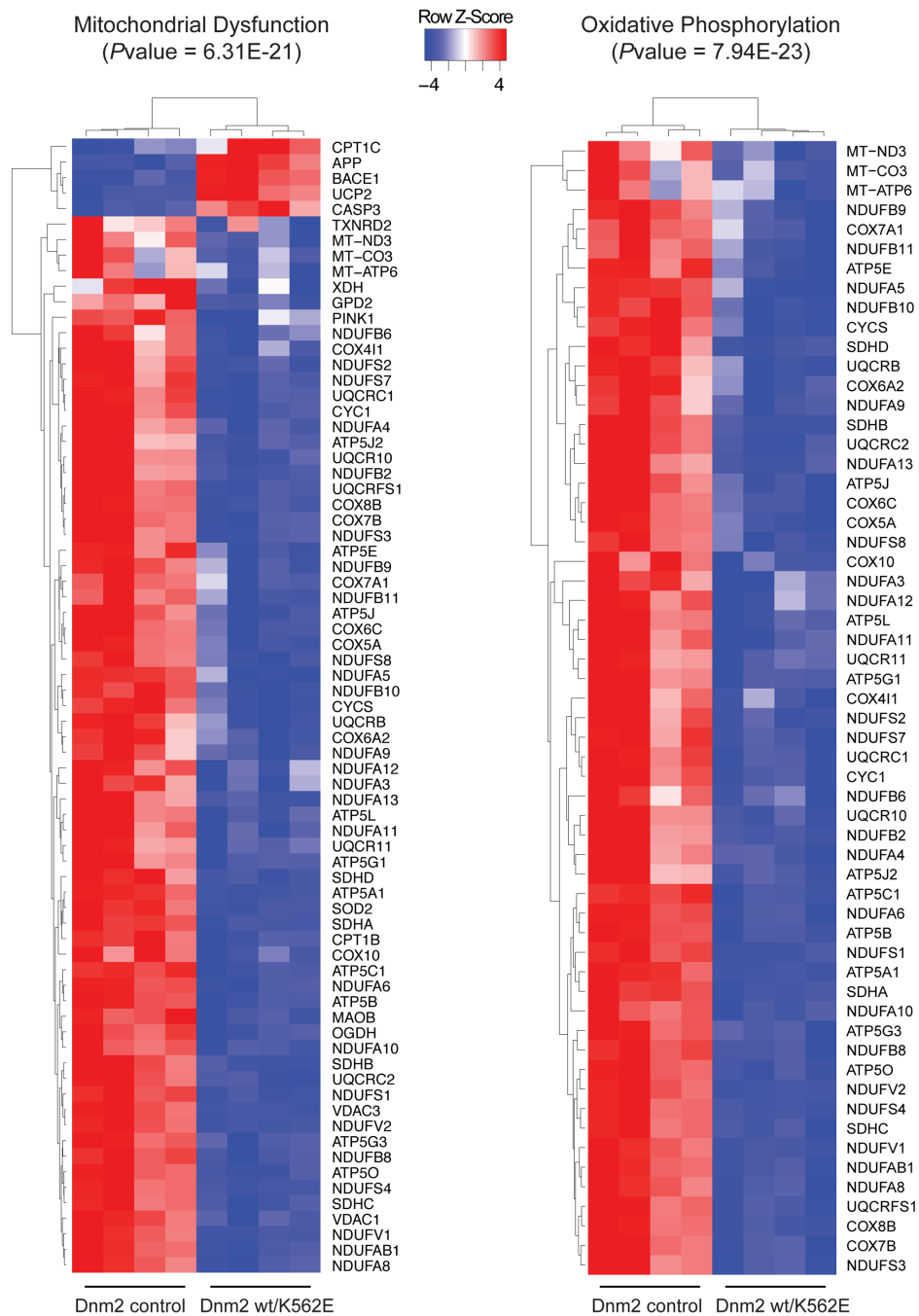




**Supplementary Material Figure S6: Checkerboard pattern of fiber-type distribution is preserved in Dnm2 wt/K562E soleus muscle.**

(A) Exemplary pictures from immunolabelled cryosections of control and Dnm2 wt/K562E soleus muscles derived from 2 months- and 1 year-old mice, probed with isotype-specific antibodies recognizing myosin heavy chains characteristic of type I, or type IIA, or type IIB myofibers. Myofibers not labelled by any of the three antibodies used are likely type IIX. Note that the red signal is also not-specifically present around fibers of all types. The checkerboard random pattern of fiber-type distribution is not disrupted in Dnm2 wt/K562E samples. (B) Quantification of the percental abundance of type I and type II (includes the type IIA and IIB) myofibers from control and Dnm2 wt/K562E soleus muscle sections (shown in A) reveals only marginal changes in the numbers of both type I and type II fibers between both genotypes. Bar heights: Mean; error bars: s.e.m. (n = 5 mice/genotype at 2 months and 1 year, images from at least 3 sections per mouse were quantified and averaged). Two-Way ANOVA with Sidak's multiple comparisons test. Significance was set at \*p < 0.05.

IPA Ingenuity Analysis - Canonical Pathways



**Supplementary Material Figure S7: IPA Ingenuity canonical pathway analysis highlights mitochondrial-related transcripts as differentially regulated in soleus muscles of Dnm2 wt/K562E versus control mice.**

IPA Ingenuity analysis of canonical pathways reveals that oxidative phosphorylation and mitochondrial dysfunction are the most significantly represented categories in the dataset (FDR < 0.05 and log2 fold change at least  $\pm 0.58$ ). Heatmap representing the transcripts associated by Ingenuity with each of these 2 canonical pathways confirms they are dominantly downregulated in Dnm2 wt/K562E compared to control soleus muscles (n = 4 mice/genotype).

